Hydrothermal Dolomitization on Devonian to Carboniferous Carbonates in Kinta Valley, Perak, Malaysia: A Petrographic Study

Nurul Afiqah Mohammad Zahir, Mirza Arshad Beg, and Askury Abdul Kadir

Department of Geosciences, Universiti Teknologi PETRONAS, Perak, Malaysia

Corresponding author: : afiqahzahir94@gmail.com, arshad.mirza@utp.edu.my
Manuscript received: December, 15, 2018; revised: February, 7, 2018;
approved: September, 18, 2019; available online: January, 31, 2020

Abstract - Thick Devonian carboniferous carbonates had been deposited in a shallow marine before they were uplifted by granitic intrusion during Triassic. This carbonate platform was selectively dolomitized along N-S oriented deep-seated fault that presented in the carbonate platform. Dolostones are characterized into significant matrix dolomites and several cement dolomites. In petrography point of view, matrix dolomites comprise very fine- to fine-crystalline nonplanar-anhedral dolomite (Dolo-I), fine- to coarse-crystalline nonplanar-anhedral to planar dolomite (Dolo-II), and fine- to medium-crystalline planar- dolomite (Dolo-III). Cement dolomites also consist of medium- to coarse-crystalline planar saddle dolomite (Dolo-IV) which halfway or totally fill disintegration vugs and breaks and coarse- to very coarse-crystalline nonplanar to planar dedolomite (Ded-I). Matrix dolomites predated cement dolomites, later infilled with sepiolite and calcite. The origins of matrix and cement dolomites and other diagenetic minerals are interpreted based on the petrography and isotopic signatures by a previous worker. Dolo-I dolomite was initiated by the early stage of dolomitization with the replacement of calcite by first driving fluids from low to high temperature of magmatic source. While Dolo-II dolomite was formed with slightly modified from Dolo-I and more Mg concentration inputs. Dolo-III dolomite was likely the consequence of hydrothermal fluids causing a brecciation textures as dolomite precipitated rapidly. Subsequently, in a high temperature, the Dolo-III dolomite was formed by precipitation of cement dolomite, hydrothermal fluids as evidenced by highly depleted values of isotopic $\delta^{18}O$. This study intends to provide useful information for understanding the dolomitization processes in alteration of hydrothermal related to Palaeozoic carbonates within Kinta Limestone.

Keywords: dolomite textures, hydrothermal dolomite, paragenetic sequence, Kinta limestone

Introduction

Dolomites have widely used in the world economic industry and also as one of reservoirs in petroleum system to discover hydrocarbon. The charateristics of dolomite with high porosity and permeability make a certain dolomite rock be a good reservoir. In this case, the origin and the impact of dolomite formation in limestone still need to be discussed by identifying the main factor of this rock formation. The key parameters control appropriation of rock heterogeneities in dolomites, which in the long run control the reservoir quality. Yet, they are still inadequately seen, particularly in those subsequent form from deficiency fault-controlled or other related replacement forms (for example Duggan *et al.*, 2001; Wilson *et al.*, 2007; Sharp *et al.*, 2010).

For Kinta Limestone, the metamorphic and diagenetic alterations that affect the complex of stratigraphy, are the significant potential on the modern use of limestone containing tin mineralization (Gebretsadik *et al.*, 2015; as cited in Anua and Zabidi, 2018). The limestone was believed to be recrystallized due to metamorphism of granitic intrusions (Khoo and Tan, 1983; Hutchison, 1994) and other diagenesis phases (Foo, 1983; Hutchison, 1975 and 1994) to change into marble and dolomite. In this case, Kinta Limestone outcrop constitutes an example of fault-controlled hydrothermal dolomitization. Besides, some studies have discovered and proved that the dolomite of Kinta Valley occurred from deep-seated dolomitization fluids (Shah *et al.*, 2018). However, there is no detailed work that has been done on the paragenesis of the dolomite rocks. In this paper, detailed petrographic examinations (microscope optical and cathodoluminescence) were completed on the hand-specimen dolomite samples taken from the Palaeozoic Kinta Limestone. This study aims to produce a diagenetic paragenesis of the dolomite in the studied area. The importance of this study is to give a general idea of how dolomite forms in limestone without going through a normal diagenesis of a sedimentary rock.

Geology and Tectonics of Kinta Valley

The studied area is located in the central part of Perak (Figure 1). The age range of Kinta Valley is Devonian to Permian where most of these sedimentary rocks are in the Devonian age (Rajah, 1979). Ingham and Bradford (1960) dated the age of Kinta Limestone as Carboniferous, but later, Foo (1983) proposed that the age range of this limestone was from Silurian to Permian. Then, Metcalfe (2000) established a stratigraphic scheme of Kinta Valley with the estimation age of Kinta Limestone and Saiong Beds (Figure 1). In Peninsular Malaysia, Kinta Valley is situated in the western belt, and it is characterized by the presence of many remnant karstic limestone hills bordered by two ranges

which are Kledang Range in the west and the Main Range in the east.

Thermal and regional metamorphism which is caused by the intrusion of granitoids and the earth movements that preceded and continued during and after the granitic emplacement, have affected the sedimentary rocks (Rajah, 1979). The residual hydrothermal fluids, rich in ores like cassiterite (tin), are emitted from the cooling granitic magma into fractures and faults that are present in abundance close to the contact of the granite and limestone (Choong *et al.*, 2014). Kinta Valley is underlain by clastic sedimentary rocks such as interbedded sandstone, mudstone, and shale, besides granite and limestone (Choong *et al.*, 2014).

In the studied area, Rajah (1979) grouped major lithologies into six types of rock; (1) calcareous rock, (2) argillaceous rock, (3) arenaceous rock, (4) tourmaline-corundum rock, (5) granitoid, and (6) alluvium. Then, a further study about geological features of Kinta Valley made by Choong *et al.* (2014) divided them into five types, which are; (i) granite, (ii) interbedded sandstone and mudstone, (iii) shale, (iv) limestone, and (v) alluvium. For nonsedimentary rocks like schist and shale, Ingham and Bradford (1960) classified them as argillaceous facies in calcareous series and dated them as carboniferous.

Malay Peninsula frames are as parts of the SE Asian continental centre of Sundaland (Metcalfe, 2011a; 2011b; 2013), comprising two blocks that were amassed by Late Triassic Sibumasu Terrane (west part) and Sukhothai Arc (East Malaya Block). The division between the Sibumasu Terrane (Western Belt) and the Sukhothai Arc (Central and Eastern Belts) (Figure 1) was framed from the Bentong-Raub suture zone and subduction underneath the Indochina Block or Sukhothai Arc. They have obliterated remainders of the Devonian-Permian principle Palaeo-Tethys sea basin, which created the Permian–Triassic andesitic volcanism and I-Type granitoids as seen in the Central and Eastern Belts of the Malay Peninsula (Metcalfe, 2013).

At the Western Belt, the Main Range granite together with the substantial scale folding of the
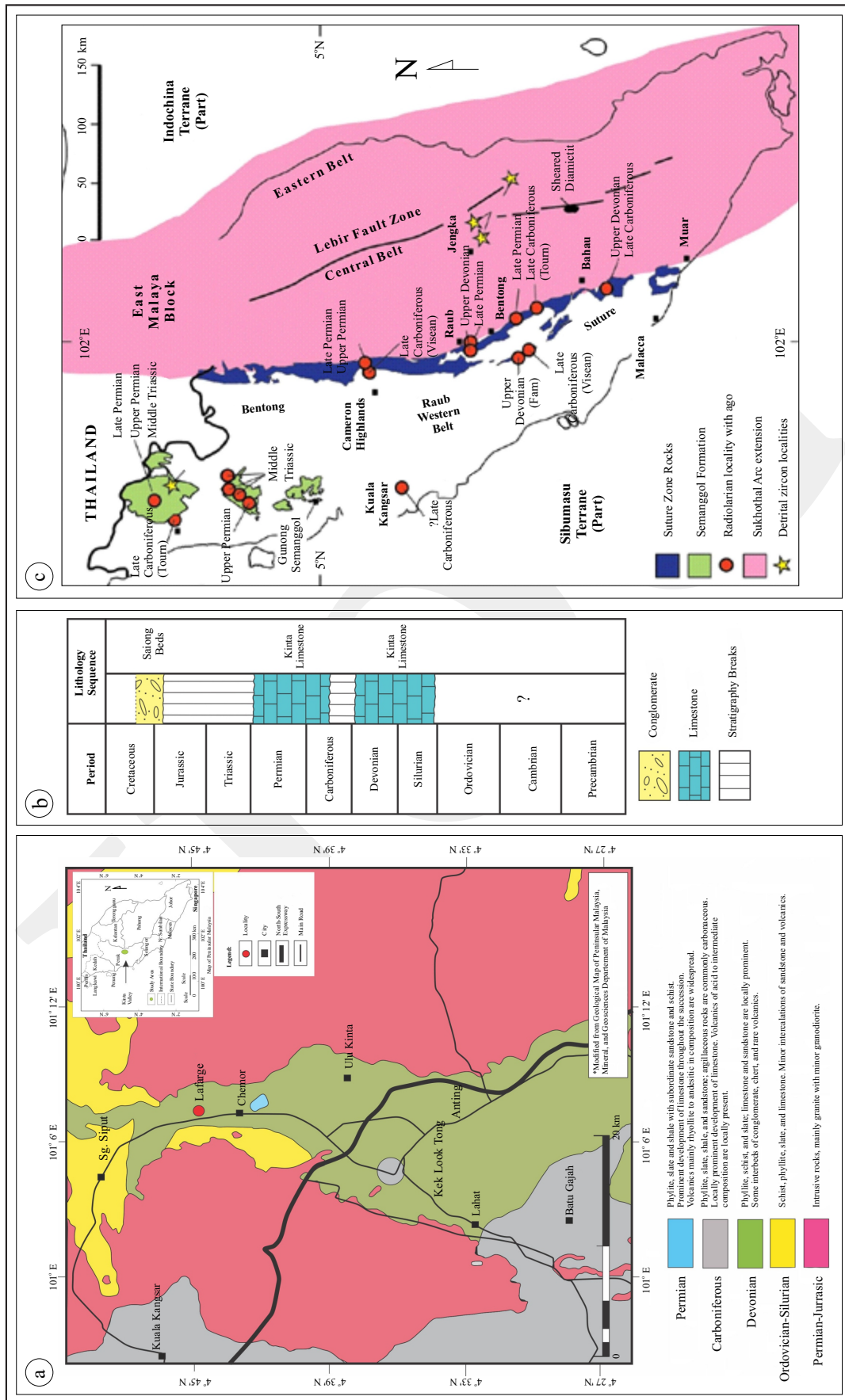
Figure 1. (a) Geological map of Kinta Valley shows the location of the studied area in the middle part of Perak. (b) A regional stratigraphy column of Kinta Valley (Modified from Metcalfe, 2000). (c)The conveyance of the Palaeo-Tethys Bentong-Raub Suture Zone and Semanggol Formation in the Malay Peninsula comparing distribution of sedimentary and metasedimentary rocks in Sibumasu Terrane and Sukhothai Arc with another terranes/blocks (from Metcalfe, 2000, 2011a, 2011b; Zhu *et al.*, 2011; Hall and Sevastjanova, 2012).

sedimentary units produce a highly fractured and pursued by the exhumation of the granite bodies amid the late Early Cretaceous and Early Cenozoic (Krähenbuhl, 1991; Cottam *et al.*, 2013; Md. Ali *et al.*, 2016; François *et al.*, 2017; Sautter *et al.*, 2017). They likewise suggested that moving liquids in the Late Cretaceous brought a significant remagnetiz ation of Palaeozoic and Triassic rocks (Metcalfe, 1993, 2013; Richter *et al.*, 1999; Ramkumar *et al.*, 2019). In the Main Range granitoids, during Late Cretaceous, thermal episodes may be presented by huge acidic or felsic fluids stopping up existing structure sets (Sautter *et al.*, 2017). As reported, in Late Cretaceous a thermal occasion was derived as bringing about recrystallization and dolomitization of parts in the Kinta Limestone (Suntharalingam, 1968; Foo, 1983; Wong, 1991; Fontaine and Ibrahim, 1995; Lee, 2009).

Methodology

Samples were collected based on a horizontal systematic sampling technique by using a geological hammer during the geological fieldwork in 2018, for a detailed petrographic analysis and interpretation. Samples were also collected in a hand specimen size about 10 to 15 cm. During the fieldwork, HCl acid was used to distinguish between limestone and dolomite. A huge emitted bubbles and released gas can usually be seen from the fast reaction between HCl and limestone, while dolomite only shows a slow reaction and a little of bubble and gas released. The results of this study were from detailed interpretation of microscopic petrography and cathodoluminescence microscopy.

These methods are used to identify the characteristics of dolomite and calcite crystals under polished thin sections. All observation of physical appearance of dolomite and calcite crystals will be analyzed and reported into a few phases according to their criteria. Outcrops in Lafarge-Kathan quarry (Hill E and Hill B) were successfully described and logged (Figures 2 and 3). Petrographic characterization was performed on thirty-five hand specimens, some of the samples were selected for another detailed analysis. A detailed petrographic study was conducted on twelve polished thin sections which were stained with Alizarin Red-S and
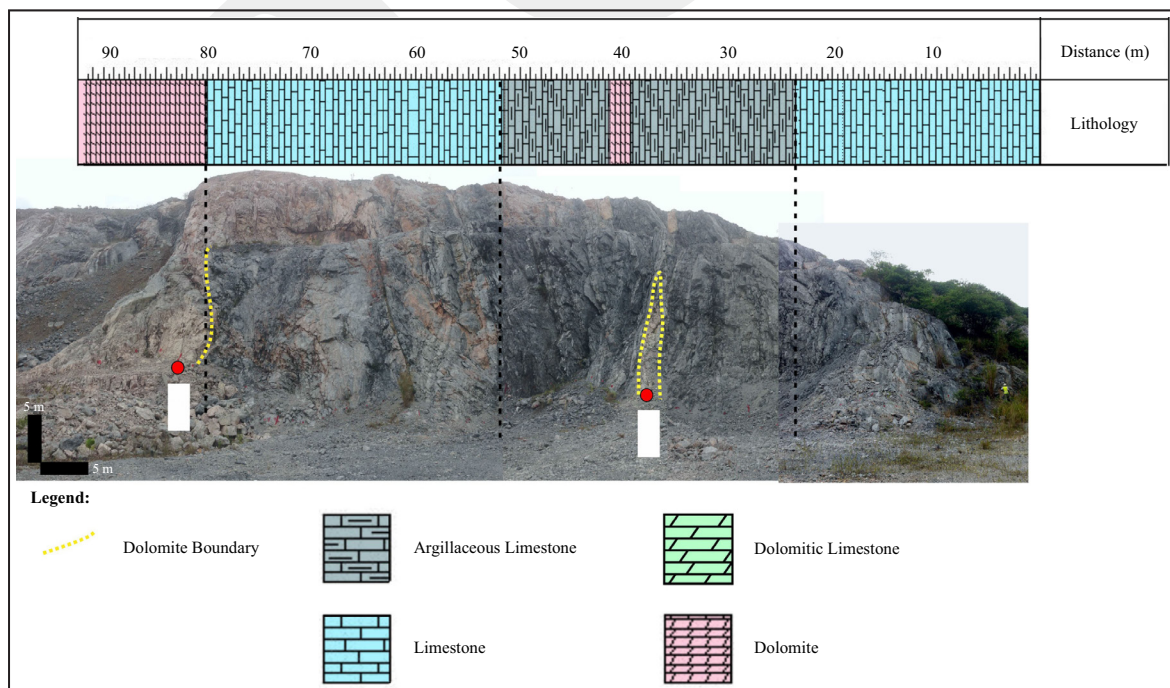

Figure 2. Outcrop image and sedimentary logging of Lafarge Hill B. From the figure, the top layer is situated on the right side of the image and roughly the thickness of the bedding is 5 to 8 cm.
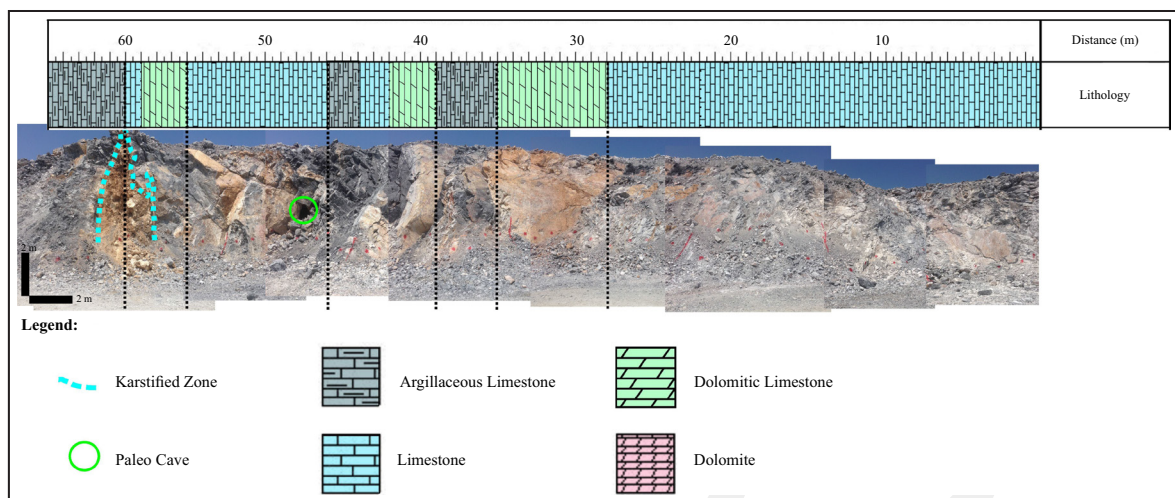
Figure 3. Outcrop image and sedimentary logging of Lafarge Hill E. The thickness of the bedding varies, but mostly in 4 to 15 cm.

potassium ferricyanide as to distinguish calcite crystals and dolomite crystals. Scanning electron microscope (SEM) analysis was also conducted on five samples at Central Analytical Laboratory (CAL), used to provide the crystal morphology. The sample size for SEM analysis is 5x10x10 mm, coated with gold. The samples were mainly selected to dolomite samples and choose samples near the dolomite boundaries. Cathodoluminescence microscopy analysis was conducted by utilizing Olympus BX43 in SEACaRL laboratory at Universiti Teknologi PETRONAS under 60μ torr and 250 Å at 12-15kV.

RESULTS

Dolomite Petrography

Based on the crystal size, distribution, and crystal surface shape (planar and nonplanar textures), there are five classification of dolomite textures made by Gregg and Sibley (1984) and Sibley and Gregg (1987) which are identified in the matrix and cement of dolomite rocks from the Palaeozoic Kinta Limestone. Matrix dolomites are composed of: (i) very fine- to fine-crystalline nonplanar-a dolomite (Dolo-I), (ii) fine- to coarse-crystalline nonplanar-a to planar-s dolomite (Dolo-II), and (iii) fine- to medium-crystalline planar dolomite (Dolo-III).

Cement dolomites comprise two types of dolomite textures: (i) medium-coarse crystalline planar saddle dolomite (Dolo-IV) and (ii) coarse- to very coarse-crystalline nonplanar to planar dedolomite (Ded-I).

Matrix Dolomite
Very fine- to fine-crystalline nonplanar-a dolomite (Dolo-I)

From hand specimen, Dolo-I dolomite is light pink in colour but some also appears in light to dark grey colour. In photomicrograph, Dolo-I dolomite crystals show a range from 50μm to 90μm in size, commonly shown as a micritic dolomite (Figure 4a). The relatively fine dolomite crystals are presented in scattered and mostly supported as a dolomite matrix of limestone clasts. The Dolo-I dolomite is relatively about 10% (volumetrically). Under cathodoluminescence light, this dolomite crystals mostly show a dull to extremely dull-red colour.

Fine- coarse crystalline nonplanar-a to planar-s dolomite (Dolo-II)

This type of dolomite appears as grey to light pink colour in hand samples. Under thin section, these dolomite crystals show 90μm to 500μm in crystal size which indicate a nonplanar-a to planar-s textures (Figures 4b and 4c). Commonly, dolomite crystals have moderate to irregular and curvy crystal surfaces; tightly-packed crystal
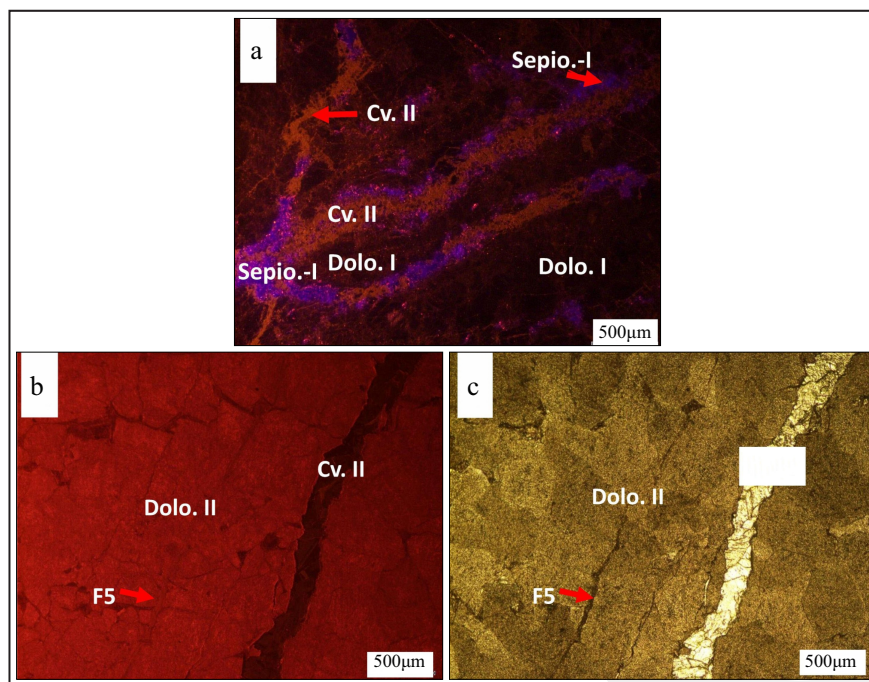
Figure 4. Photomicrographs of matrix dolomites. (a) Matrix dolomites, Dolo-I dolomite crystals - fine nonplanar, anhedral dolomite crystals with calcite cementation filled into fracture/vugs, under CL. (b and c) Paired photomicrographs of Dolo-II dolomites: fine- to coarse-crystalline nonplanar, anhedral to planar-subhedral dolomite crystals tightly packed and interlocking dolomite crystals, under plane-polarized light (b) and under CL (c).

mosaics with almost absence of intercrystalline pores. Generally, this dolomite type is fabric-destructive and as original depositional and/or early diagenetic features clearly undistinguished (Guo *et al*., 2016). Also, Dolo-II mostly has a cloudy appearance on surfaces with extremely rare clear rim that can be observed under thin sections. Some of the remaining spaces of pore are either open or later infilled by calcite crystals. Generally, the transition between calcite crystal and Dolo-II dolomite crystal is abrupt. Under cross-polarized light, it commonly shows an undulatory extinction and also displays dull-red luminescence under CL. This dolomite type is present in the Lafarge Hill B but roughly makes up less than 10% of the dolomites.

Fine- to medium-crystalline planar dolomite (Dolo-III)

Dolo-III dolomite type is typically shown by a light pink to pink colour. They are easy to distinguish with the darker colour of dolomite crystals compared with the pinkish colour of limestone (Figure 5a). Under thin sections, the

sizes of Dolo-III dolomite crystals are commonly 60 to 600μm, exhibit as patchy or a bit mottled appearance and floating (Figure 5b) in the dominant micrite dolomite matrix with the presence of a clast of limestone. Also, these dolomite type crystals are mostly present as euhedral and subhedral crystal shapes and large crystals which generally have a cloudy centre surrounded by a darker rim. Under observations of cross-polarized light, these dolomite crystals display a sharp or slightly undulatory extinction. For observations under CL, they display a bright to dull-red luminescence centres with nonluminescent rim. The Dolo-III dolomite is typically present only in a brecciated limestone within dolomites from Lafarge Hill E, comprising approximately 5% dolomite rocks in volume.

Cement Dolomite

Coarse crystalline planar saddle dolomite (Dolo-IV)

This Dolo-IV dolomite is commonly creamy white or pink in colour in hand specimen and partially or completely filling the vugs and/or frac-
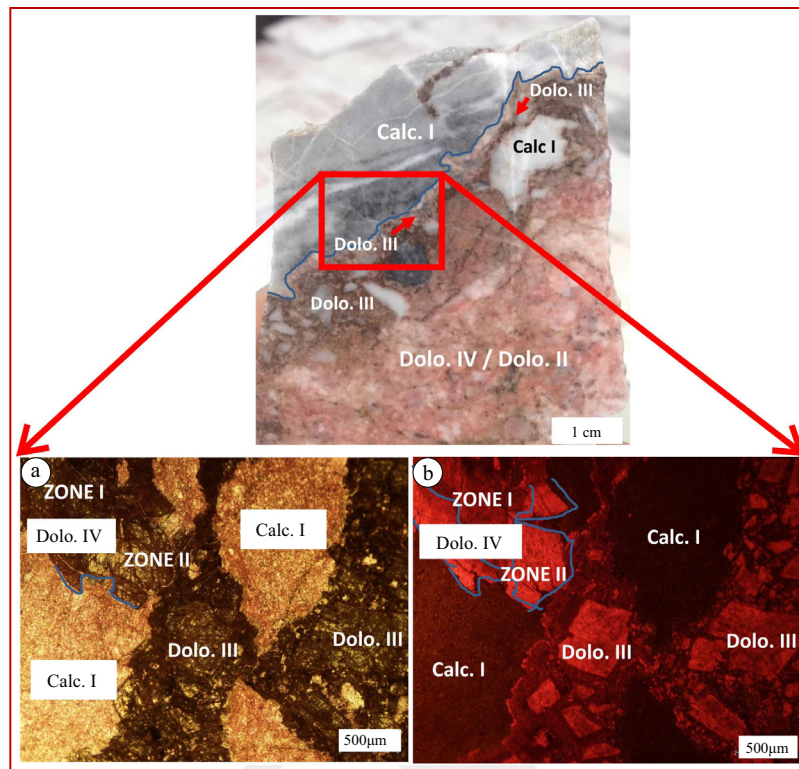
Figure 5. A photomicrograph of Dolo-III dolomites. Top image shows the brecciation and contact between host limestone and dolomite cements in hand specimen of Lafarge Hill E. (a) A photomicrograph of Dolo-III in plane-polarized light which shows limestone clasts displaying pink and dark brown colours for dolomite matrix. (b) Photomicrograph of Dolo-III under CL shows a little mottled appearance and displays bright to dull-red luminescent centres and nonluminescent rim dolomite crystals.

tures. In thin section, Dolo-IV dolomite crystals are 200 µm to 1000 µm in size (Figure 6a), commonly have scimitar-like (curvy shape that broadens towards the point in Figure 6b) terminations with curved or lobate crystal surfaces. They occur as the outermost cement lining the smooth to dissolution vugs and mouldic pores in the matrix dolomites (Figures 6c and 6b). Mostly they display sweeping extinction under cross-polarized light. Under CL, these dolomite crystals exhibit similar dull- red luminescence to that of the matrix dolomites, with thin to thick clear rims showing a brighter-red luminescence. The Dolo-IV dolomite crystals mostly occur as the first generation of cements, but some are found growing over and forming a zonation. The pore spaces that remain unfilled are either open and/or filled by late cementation of calcite crystals. However, the transition between Dolo-IV dolomite and later calcite crystals that can be observed is extremely rare. Mostly remaining pore spaces are open without having any infilling calcite

crystals. Volumetrically, the Dolo-IV dolomite only constitutes more than 5% of the dolomite rocks.

Coarse- to very coarse-crystalline nonplanar to planar Dedolomite (Ded-I)

In hand samples, this dolomite type is commonly in light pink to brown colour. In crystal size, this Ded-I dolomite type has 400µm to 1,200µm and exhibits a planar subhedral to nonplanar crystals. Besides, in the inner parts, the dolomite crystals have a dark centre, thick cloudy, slightly sweeping extinction in polarized light (Figures 6d and 6e). In CL petrography, cloudy and dark centres display a dark-red luminescence to nonluminescence. A hole and embayed surfaces can be observed on the crystal surfaces. There might occur cementation of Dolo-IV and/or later replacement of calcite crystal resulted in a partial to complete occlusion of crsytal surfaces. Generally, this dolomite is not a typical type to be found, and it consits only of 1% which presents in the dolomite rocks.
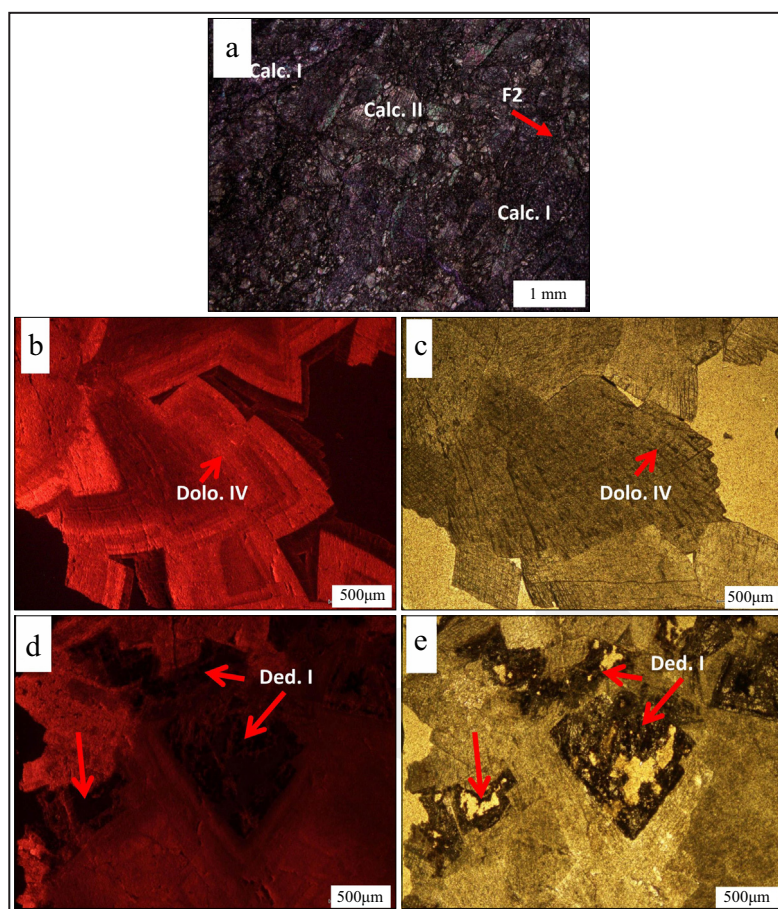
31

Figure 6. Photomicrographs of cement dolomites. (a) Stained thin section for host limestone in Hill E, present a micrite and blocky calcite cements under plane polarized light. (b) Dolo-IV under CL which showing a zoned saddle dolomite, coarse planar e(s) dolomite cementation with partially or completely overgrowth in vugs and/or fractures. (c) Same photomicrograph of (b) under plane-polarized light. (d and e) Ded-I dolomite cements which dissolution and replacement of other phases occurs at the centripetal of crystal forming a dark cores (red arrow).

Dolomite Morphology

From the previous section, some of the dolomite petrography exhibit a nonplanar-a texture with medium- to coarse-dolomite crystals in size. The FESEM results in Figure 7 revealed that the dolomite morphology in this area has two types. The main morphology that was observed under FESEM micrograph is anhedral shape or angular with sharp edges and/or curved surfaces (Figure 7a). The grain size varies from 5μm to 100μm. Besides, a rhombohedral shape morphology (Figure 7b) of dolomite grain is also found in the samples. This morphology is very minor, and generally the grain size is 2μm up to 15μm which is very small. Micrographically, some parts of the samples show open spaces or small intercrystalline pores, but are very low amount.

Paragenetic Sequence

From detailed hand specimen descriptions of microscopic studies and the paragenetic sequence of matrix dolomites and cement dolomites closely-associated fracture- and vug-filling have finalized and illustrated in Table 1. The stages of early and intermediate diagenesis are described relative to stylolite formation (Qing and Mountjoy, 1989, 1994; Chen et al., 2004). Micrite and blocky calcite cements must have developed during early diagenetic products of the formed limestone, and stylolite formation also occurred earlier to dolomitization. The occurrence of stylolite for Stylo-I is generally considered to occur during the diagenesis transition from early to intermediate stage (Qing and Mountjoy, 1989, 1994; Tucker and Wright, 1990; Chen et al., 2004;
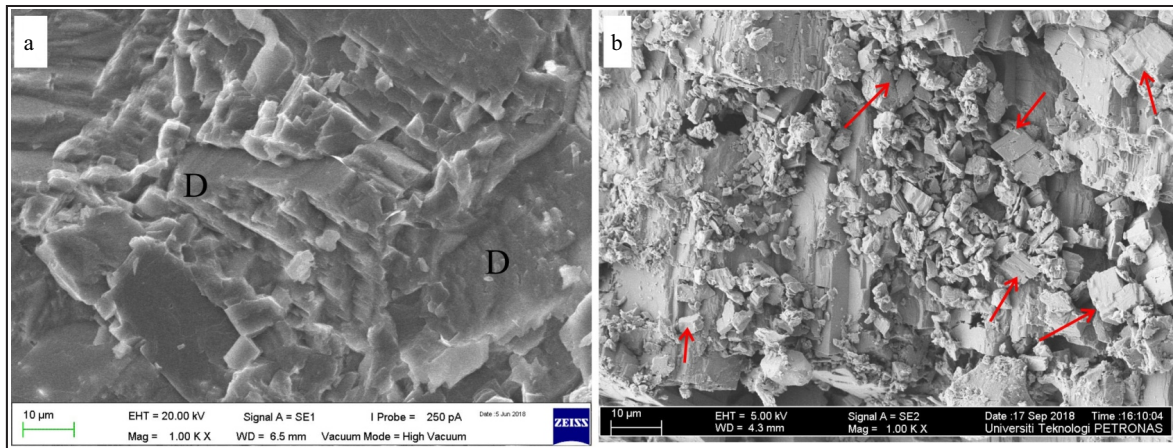
Figure 7. (a) Photomicrograph of SEM shows the flakes and sharp edges of dolomites, with no clear boundaries between one another. (b) The red arrow in the photomicrograph shows the dolomite grain that exhibits in a perfect rhomb shape.

Table 1. Paragenetic Sequence of Devonian to Carboniferous Carbonates (the Kinta Limestone Formations) in the Studied Area based on Hand Specimen and Petrographic Analyses

Diagenetic event	Diagenetic Stages		
	Early	Intermediate	Late
Micritic to equant cement (Calc-I)	▬		
Blocky calcite cements (Calc-II)	▬		
Vein calcite 1 (Cv I)	▬		
Stylolization (Stylo-I)	▬▬ ▬▬		
Early fracturing- (F1, F2)	▬		
V. Fine- fine, anhedral nonplanar, -a (Dolo-I)		▬	
Second Fracturing- (F3, F4)		▬	
Vein calcite 2 (Cv-II)		▬	
Fine- to coarse, nonplanar-a (Dolo-II)		▬	
Third fracturing- (F5, F6)		▬	
Vein calcite 3 (Cv-III)		▬	
Fine-medium, Fine-medium, planar (Dolo-III)		▬	
Coarse-V. Coarse, nonplanar-a to plamar-s (Dolo-IV)			▬
Coarse, dedolomite (Ded-I)			▬
Sepiolite occurrence 1 (Sepio-I)			▬
Vein calcite 4 (Cv-IV)			▬
Late fracturing- (F7,F8)			▬

Note: The blue boxes are the estimation of duration whether long period (long boxes) or short period (small boxes) for each phase in this paragenetic sequence. The diagenesis for initial, intermediate, and late stages are stated based on the formation of stylolites and fractures.

Ronchi *et al*., 2011; as cited in Jacquemyn *et al*., 2014). Matrix-dolomites are clarified to be the early stage of dolomitization as indicated by the presence of Dolo-I dolomites replacing micritic calcite cements of host-limestones.

The occurrence of Dolo-II dolomite with coarser texture in the middle of Dolo-I dolomite crystal cements indicates recrystallization which postdated fine matrix dolomite. The created porosity together with a new fracturing event

after Dolo-II formation could have made a new dolomitizing and mineralizing fluid-flow channel; and they contributed to the formation of more porosity and void-filling dolomitization producing saddle dolomite cements (Dolo-IV). For Dolo-III, limestone clasts with stained pink colour appear unaltered without any sign of dolomitization. Limestone-breccia bodies are millimetre to centimetre in size and show irregular shapes. These features and the unaltered limestone clasts imply

a repeated rapid brecciation and cementation processes in which dolomitization only took place in the fracture porosity enhanced by over pressured fluids (Lopez *et al.*, 2010).

The fracturing event after Dolo-II formation have promoted the last dolomitizing fluid pulse which was responsible for the precipitation of planar-e(s) (Dolo-III). A late stage of dissolution of Ded-I dolomite crystal might a result of dolomite alteration by meteoric water or replaced by another mineral phase. A late stage of mineralization and calcitization, including sepiolite minerals (Sepio-I), calcite veins, and fractures that cross cut the previous phases (F7 and F8) postdated all dolomites.

DISCUSSION

Origin of Matrix Dolomites

The majority of Dolo-I is very fine- to fine-crystalline matrix (50-90 µm) with nonplanar-a textures, which relatively forms in low temperatures and links to penecontemporaneous to near-surface dolomitization (Gregg and Sibley, 1984; Sibley and Gregg, 1987; Gregg and Shelton, 1990; Al-Aasm and Packard, 2000; Warren, 2000; Machel, 2004; as cited in Guo *et al.*, 2016). The closely-packed nonplanar, fine to coarser crystal behaviour of Dolo-II dolomites suggest that this texture type was forming at higher temperatures due to rapid disorder crystal growth which was apparently above the roughening temperature (Gregg and Sibley, 1984; Gregg and Shelton, 1990; Montanẽz and Read, 1992; Chen *et al.*, 2004).

Generally, the critical roughening temperature (50 - 60⁰C) and above are more favoured for nonplanar texture type of dolomite crystals to form (Gregg and Sibley, 1984; Sibley and Gregg, 1987). However, this type of dolomite crystals could also form at lower temperatures with supersaturated fluids (Gregg and Sibley, 1984; Sibley and Gregg, 1987; Warren, 2000; Meister *et al.*, 2013, as cited in Gou *et al.*, 2016). In addition, according to Guo *et al*. (2016) dolomite crystals

under cathodoluminescence light that display a dull to extremely dull luminescent might show the existence of Fe^{2+} in the fluids where it was early precipitated (Pierson, 1981; Machel and Burton, 1991; Richter *et al.*, 2003; Vuillemin *et al.*, 2011).

Moreover, coaser dolomite crystals with bright luminescent surrounded by non-luminescence irregular fine dolomite (Dolo-IV) show a later precipitation and extra Mn concentration in the fluids through precipitation (Pierson, 1981; Machel and Burton, 1991; Richter *et al.*, 2003; Vuillemin *et al.*, 2011). The appearance of breccia texture in Dolo-III dolomite type implies a stress relief impacted from hydrofacturing, whereas the fractures were forced by upward over pressure hydrothermal fluids (Davies and Smith, 2006). This phenomenon would look like the explosive of rocks into the fluids. Besides, the isotopic analysis of fine- to medium-crystalline matrix dolomite supports that these types of dolomite are of hydrothermal origin since they show a highly depleted $\delta^{18}O$ values ranging from -13.75‰ to -11.10‰ VPDB (Shah *et al.*, 2018). For instance, the values of $\delta^{18}0$ are slightly more depleted than other analyzed hydrothermal dolomites like those of western Canada, Guilin, and Southern Cantabrian Zone, Spain, which show the values of $\delta^{18}O$ ranging from -13.9‰ to -3.5‰ (Shukri, 2010).

Origin of Cement Dolomites

As stated before, two classes of cement dolomites are identified in the studied area: planar-e(s) (Dolo-IV) and nonplanar to planar-s saddle dolomite (Ded-I). For Dolo-IV dolomite crystals, their presence as cement infilling fractures and associated vugs indicates that their precipitation and cementation were closely associated with fractures or tectonic activity to widespread areas. In this particular subject, the fluids from the bottom (at depth) could already provide pathways to rift upwards using open structures. Then, with respect to the dolomite, as Mg content in hydrothermal fluids gains the level of saturation, there will be a precipitation of dolomite crystals from the fluids and develop along the structures and voids (Dong *et al.*, 2013; as cited in Guo *et al.*, 2016).

Apparently, Dolo-IV experiences a coarsening and curving dolomite crystal with progressive overgrowth relative to Dolo-II dolomites that leads to form in high temperature and Mg inputs. At the same time, crystal coarsening (or recrystallization) of matrix dolomite could also be caused by the hydrothermal fluids and make it more precipitated rapidly (Guo *et al.*, 2016) as shown in the dolomite rock adjacent to the structure pathways, probably through thermal baking and fluid diffusion. Besides, a highly depleted $\delta^{18}O$ values of well develop and coarse-crystalline dolomite cements yield -18.75‰ to -15.04‰ VPDB indicating a hot source of dolomite cements from deep magmatic basin (Shah *et al.*, 2018). While for Ded-I dolomite crystals, dedolomitization occurred irregularly along crystallographic planes near the centripetal, and some of the de-dolomitization occurred near the boundary between the two generations of cements which most of it affected the first generation. This process commonly occurs during the dissolution of associated calcium sulfates or at a high temperature (Scholle, 2003).

Purser (1985) considered that the de-dolomitization could enlarge the dissolved moldic pore and/or intercrystal space. After dolomite dissolved, the space was filled with latter cements, forming dolomite crystal mold. The crystal moldic pore can indicate the exposure and the effect of meteoric water (Jie *et al.*, 2001). By following classification made by Jie *et al.* (2001), Ded-I probably occurred during near surface dedolomitization conditions. With high content of Ca, low Mg, low partial pressure of CO_3 and solution of below 50°C , dedolomitization that occured near surface is more often relateable with dissolution of gypsum and dolomite in vadose or phreatic meteoric water state.

vations, the dolomite bodies are more associated with N-S oriented fault system in the Palaeozoic limestone. Petrographic studies have revealed the presence of fine- and coarse-crystalline, interlocking, and saddle type of dolomite textures in the studied area. Three types of matrix dolomites and two types of cement dolomites are differentiated from hydrothermally-altered dolomites.

The process of dolomitization occured before two phases of late sepiolite and calcite cement in fractures/veins. Probably the replacement and recrystallization have formed the matrix dolomites in shallow to deep burial conditions (Guo *et al.*, 2016). But, in this case, fine-crystalline matrix dolomite shows an initial phase of replacive dolomitization, and later late stage of dolomite cementation comes and fills up the open spaces. These hydrothermal fluids have resulted in dissolution and precipitation of dolomite and proceed with matrix dolomite recrystallization. However, the high temperature of hydrothermal fluids could have formed and percipitate the cement dolomites. This will make Mg content in the fluids be very saturated and cause fluid cannibalization and migration from the underlying dolomites as there are the addition of fluid flows in.

Even though the origins of the initial phase and later phase of the dolomite have been proved by isotopic signatures from a previous work and exhibit a close relationship, they indicate a different temperature and nature of dolomitizing fluids. Host limestone (clast breccia) in dolomite cements shows the high intensity of over pressured upwelling fluids. As concluded, precipitation of hydrohermal dolomite stops to form as Mg content drops and calcite precipitates subsequently with high influx of meteoric waters.

Conclusions

This paper presents detailed hydrothermal dolomitization in the Devonian to Carboniferous limestone in the Kinta Valley. From field obser-

References

Adams, J. E., Rhodes, M. L., 1960. Dolomitization by seepage refluxion. *American Association of Petroleum Geologists, Bulletin*, 44, p.1912-1920.

Al-Aasm I.S. and Packard J.J., 2000. Stabilization of early-formed dolomite: a tale of divergence from two Mississippian dolomites. *Sedimentary Geology,* 131, p.97-108. DOI: 10.1016/S0037-0738(99)00132-3

Anua, N.E.Q.M. and Zabidi, H., 2018. Petrography and Geochemistry of Kinta Valley Palaeozoic Carbonate Rock. *Journal of Physics: Conference Series 1082 012095*. DOI: 10.1088/1742-6596/1082/1/012095

Budd, D.A., 1997. Cenozoic dolomites of carbonate islands: their attributes and origin. *Earth-Science Reviews,* 42 (1-2), p.1-47. DOI: 10.1016/S0012-8252(96)00051-7

Chen, D., Qing, H., and Yang, C., 2004. Multistage hydrothermal dolomites in the Middle Devonian (Givetian) carbonates from the Guilin area, South China. *Sedimentology,* 51 (5), p.1029-1051. DOI: 10.1111/j.1365-3091.2004.00659.x

Choong, C.M., Sautter, B., Pubellier, M., Menier, D., Weng Sum, C., and Kadir, 2014. Geological Features of the Kinta Valley. *PLATFORM-A Journal of Engineering, Science and Society,* 2 (10), p.1-14.

Cottam, M.A., Hall, R., and Ghani, A.A., 2013. Late Cretaceous and Cenozoic tectonics of the Malay Peninsula constrained by thermochronology. *Journal of Asian Earth Sciences,* 76, p. 241-257. DOI: 10.1016/j.jseaes.2013.04.029

Davies, G.R. and Smith, L.B., 2006. Structurally controlled hydrothermal dolomite reservoir facies: an overview. *American Association of Petroleum Geologists, Bulletin,* 90, p.1641-1690.

Dong, S., Chen, D., Qing, H., Zhou, X., Wang, D., Guo, Z., and Qian, Y., 2013. Hydrothermal alteration of dolostones in the Lower Ordovician, Tarim Basin, NW China: multiple constraints from petrology, isotope geochemistry and fluid inclusion microthermometry. *Marine and Petroleum Geology,* 46, p.270-286. DOI: 10.1016/j.marpetgeo.2013.06.013

Duggan, J.P., Mountjoy, E.W., and Stasiuk, L.D., 2001. Fault-controlled dolomitization at Swan Hills Simonette oil field (Devonian), deep basin west-central Alberta, Canada. *Sedimentology*, 48 (2), p.301-323. DOI: 10.1046/j.1365-3091.2001.00364.x

Fontaine, H. and Ibrahim, B.A., 1995. Biostratigraphy of the Kinta Valley, Perak. *Geological Society of Malaysia Bulletin,* 38, p.159-172.

Foo, K.Y., 1983. The Palaeozoic sedimentary rocks of Peninsular Malaysia - stratigraphy and correlation. *Proceedings, Workshop on Stratigraphic Correlation of Thailand and Malaysia* 1, p.1-19.

François, T., Md. Ali, M. A., Matenco, L., Ng, T.F., Taib, N.I., and Shuib, M.K., 2017. Late Cretaceous extension and exhumation of the Stong and Taku magmatic and metamorphic complexes, NE Peninsular Malaysia. *Journal of Asian Earth Sciences,* 143, p.296-314.

Gebretsadik, H.T., Sum, C.W. and Hunter, A.W., 2015. Preservation of Marine Chemical Signatures in Upper Devonian Carbonates of Kinta Valley, Peninsular Malaysia: Implications for Chemostratigraphy. *Proceedings of the International Conference on Integrated Petroleum Engineering and Geosciences*, p.291-312. DOI: 10.1007/978-981-287-368-2_28

Gregg, J.M. and Sibley, D.F., 1984. Epigenetic Dolomitization and the Origin of Xenotopic Dolomite Texture. *Journals of Sedimentary Petrology,* 54 (3), p.908-931.

Gregg, J.M. and Shelton, K.L., 1990. Dolomitization and dolomite neomorphism in the

back reef facies of the Bonneterre and Davis formations (Cambrian), south eastern Missouri. *Journal of Sedimentary Research,* 60, p.549-562. DOI: 10.1306/212F91E2-2B24-11D7-8648000102C1865D

Guo, C., Chen, D., Qing, H., Dong, S., Li, G., Wang, D., Qian, Y., and Liu, C., 2016. Multiple dolomitization and later hydrothermal alteration on the Upper Cambrian-Lower Ordovician carbonates in the northern Tarim Basin, China. *Marine and Petroleum Geology, 72*, p.295-316. DOI: 10.1016/j.marpetgeo.2016.01.023

Hall, R. and Sevastjanova, I., 2012. Australian crust in Indonesia. *Australian Journal of Earth Sciences,* 59, p.827-844. DOI: 10.1080/08120099.2012.692335

Hardie, L.A., 1987. Perspectives: Dolomitization: Dolomitization: a critical view of some current views. *Journal of Sedimentary Research,* 57, p.166-183. DOI: 10.1306/212F8AD5-2B24-11D7-8648000102C1865D

Hutchison, C.S., 1975. Ophiolite in Southeast Asia. *Geological Society of America Bulletin*, 86, p.797-806.

Hutchison, C.S. 1994. Gondwana and Cathaysian blocks, Palaeotethys sutures and Cenozoic tectonics in south-east Asia. *Geologische Rundschau*, 82, p.388-405.

Ingham, F.T. and Bradford, E.P., 1960. Geology and Mineral Resources of the Kinta Valley, Perak. *Federation of Malaya Geological Survey District Memoir,* 9, Malaya: Government Press.

Jacquemyn, C., El-Desouky, H., Hunt, D., Casini, G., and Swennen, R., 2014. Dolomitization of the Latemar platform: fluid flow and dolomite evolution. *Marine and Petroleum Geology,* 55, p.43-67. DOI: 10.1016/j.marpetgeo.2014.01.017

Jie, Z., Jianfeng, S., Yigang, W., Yingchu, W., Xingping, Z., and Anping, H., 2001. PS Dedolomitization: Types, Mechanism and Its Relationship to Carbonate Reservoir Properties. *Poster presentation at the AAPG Annual Convention and Exhibition, Houston, Texas, April.*

Khoo, T.T. and Tan, B.K., 1983. Geological evolution of Peninsular Malaysia. *Proceedings of a workshop on stratigraphic correlation of Thailand and Malaysia.* The Geological Society of Thailand and the Geological Society of Malaysia, p. 253-290.

Krähenbuhl, R., 1991. Magmatism, tin mineralization, and tectonics of the Main Range Malaysian Peninsula: consequences for the plate tectonic model of Southeast Asia based on Rb-Sr, K-Ar and fission track data. *Geological Society of Malaysia Bulletin,* 29, p.1-100.

Land, L.S., 1980. The isotopic and trace element geochemistry of dolomite: the state of the art. *In*: Zenger, D.H., Dunham, J.B., Ethington, R.L. (eds), *Concepts and Models of Dolomitization, 28, SEPM Special Publication.* p.87-110.

Land, L.S., 1985. The origin of massive dolomite. *Journal of Geological Education,* 33, p.112-125. DOI: 10.5408/0022-1368-33.2.112

Le Maitre, R.W., 1976. The chemical variability of some common igneous rocks. *Journal of Petrolology,* 17, p.589-598. DOI: 10.1093/petrology/17.4.589

Lee, C.P., 2009. Palaeozoic stratigraphy. *In:* Hutchison, C.S. and Tan, D.N.K. (eds.), *Geology of Peninsular Malaysia*. University of Malaya and Geological Society of Malaysia, Kuala Lumpur, p.55-86.

López-Horgue, M.A., Iriarte, E., Schröder, S., Fernández-Mendiola, P.A., Caline, B., Corneyllie, H., and Zerti, S., 2010. Structurally controlled hydrothermal dolomites in Albian carbonates of the Asón valley, Basque Cantabrian Basin, Northern Spain. *Marine and Petroleum Geology,* 27 (5), p.1069-1092. DOI: 10.1016/j.marpetgeo.2009.10.015

Machel, H.G., 2004, Concepts and models of dolomitization: A critical reappraisal, *In*: Braithwaite, C.J.R., Rizzi, G., and Drake, G. (eds.), *The geometry and petrogenesis of dolomite hydrocarbon reservoirs: Geological Society of London Special Publication, 235*, p.7-63, DOI: 10.1144/GSL.SP.2004.235.01.02.

Machel, H.G. and Burton, E.A., 1991. *Factors governing cathodoluminescence in calcite and dolomite, and their implications for studies of carbonate diagenesis*. Book Chapter published 1991 in Luminescence Microscopy and Spectroscopy Qualitative and Quantitative Applications. DOI: 10.2110/scn.91.25.0037

Md. Ali, M.A., Willingshofer, E., Matenco, L., Francois, T., Daanen, T.P., Ng, T.F., Taib, N.I., and Shuib, M.K., 2016. Kinematics of post-orogenic extension and exhumation of the Taku Schist, NE Peninsular Malaysia. *Journal of Asian Earth Sciences,* 127, p.63-75. DOI: 10.1016/j.jseaes.2016.06.020

Meister, P., Mckenzie, J.A., Bernasconi, S.M., and Brack, P., 2013. Dolomite formation in the shallow seas of the Alpine Triassic. *Sedimentology,* 60 (1), 270-291. DOI: 10.1111/sed.12001

Metcalfe, I., 1993. Permian conodonts from the Raub Gold Mine, Pahang, Peninsula Malaysia. *Warta Geologi*, 19, p.85-88.

Metcalfe, I., 2000. The Bentong-Raub Suture Zone. *Journal of Asian Earth Sciences*, 18, p.691-712.

Metcalfe, I., 2011a. Palaeozoic-Mesozoic history of SE Asia. *In*: Hall, R., Cottam, M., Wilson, M. (eds), The SE Asian Gateway: History and Tectonics of Australia - Asia Collision. *Geological Society of London Special Publications,* 355, p.7-35. DOI: 10.1144/SP355.2

Metcalfe, I., 2011b. Tectonic framework and Phanerozoic evolution of Sundaland. *Gondwana Research,* 19, p.3-21. DOI: 10.1016/j.gr.2010.02.016

Metcalfe, I., 2013. Tectonic Evolution of the Malay Peninsula. *Journal of Asian Earth Sciences,* 76, p.195-213. DOI: 10.1016/j.jseaes.2012.12.011

Morrow, D.W., 1982. Diagenesis 2. Dolomite: Part 2. Dolomitization models and ancient dolostones. *Geoscience Canada,* 9, p.95-107.

Montañéz, I.P., Read, J.F., 1992. Fluid-rock interaction history during stabilization of early dolomites, Upper Knox Group (Lower Ordovician), US Appalachians. *Journal of Sedimentary Research,* 62, p.753-778. DOI: 10.1306/D42679D3-2B26-11D7-8648000102C1865D

Pierson, B.J., 1981. The control of cathodoluminescence in dolomite by iron and manganese. *Sedimentology,* 28, p.601-610. DOI: 10.1111/j.1365-3091.1981.tb01924.x

Purser, B.H., 1985. Dedolomite Porosity and Reservoir Properties of Middle Jurassic Carbonates in the Paris Basin, France. *Carbonate Petroleum Reservoirs,* p.341-355. DOI: 10.1007/978-1-4612-5040-1_22.

Qing, H. and Mountjoy, E.W. 1989. Multistage dolomitization in Rainbow buildups, Middle Devonian Keg River Formation, Alberta, Canada. *Journal of Sedimentary Petrology,* 59, p.114-126. DOI: 10.1306/212F8F30-2B24-11D7-8648000102C1865D

Qing, H. and Mountjoy, E.W. 1994. Formation of coarsely crystalline, hydrothermal dolomite reservoirs in the Presqu'ile Barrier, Western Canada Sedimentary Basin. *American Association of Petroleum Geologists Bulletin,* 78, p.55-77. DOI: 10.1306/bdff9014-1718-11d7-8645000102c1865d

Rajah, S.S., 1979. The Kinta Tinfield, Malaysia. *Bulletin of Geological Society of Malaysia,* 11, p.111-136. DO: 10.7186/bgsm11197905

Ramkumar, M., Siddiqui, N.A., Mathew, M., Sautter, B., Hui, P.X., Nagarajan, R., Bre and Poppelreiter, M., 2019. Structural controls on polyphase hydrothermal dolomitization in the Kinta Valley, Malaysia: Paragenesis and regional tectono-magmatism. *Journal of Asian Earth Sciences*. 174, p.364-380. DOI: 10.1016/j.jseaes.2019.02.004

Richter, B., Schmidtke, E., Fuller, M., Harbury, N., and Samsudin, A.R., 1999. Palaeomagnetism of Peninsular Malaysia. *Journal of Asian Earth Sciences,* 17, p.477-519. DOI: 10.1016/S1367-9120(99)00006-1

Richter, F.M., Davis, A.M., DePaolo, D.J., and Watson, E.B., 2003. Isotope fractionation by chemical diffusion between molten basalt and rhyolite. *Geochimica et Cosmochimica Acta,*

67 (20), p.3905-3923. DOI: 10.1016/S0016-7037(03)00174-1

Ronchi, P., Jadoul, F., Ceriani, A., Di Giulio, A., Scotti, P., Ortenzi, A., and Fantoni, R., 2011. Multistage Dolomitization in an Early Jurassic Platform (Southern Alps, Italy): insights for the distribution of massive dolomitized bodies. *Sedimentology,* 58, p.532-65. DOI: 10.1111/j.1365-3091.2010.01174.x

Sautter, B., Pubellier, M., Jousselin, P., Dattilo, P., Kerdraon, Y., Choong, C.M., and Menier, D., 2017. Late Paleogene rifting along the Malay Peninsula thickened crust. *Tectonophysics,* 710, p.205-224. DOI: 10.1016/j.tecto.2016.11.035

Scholle, P.A., and Ulmer-Scholle, D.S., 2003. A Color Guide to the Petrography of Carbonate Rocks: Grains, textures, porosity, diagenesis: *AAPG Memoir, 77, American Association of Petroleum Geologists,* Tulsa, Oklahoma, U.S.A., p.371-392. DOI: 10.1017/S0016756800041881

Shah, M.M., Poppelreiter M.C., Kadir, A.A., and Choong, C.C., 2018. Basement associated diagenetic modifications in the Upper Carboniferous -Lower Permian Kinta Limestone (perak, Malaysia): Field/microscopic observations, isotopic signatures and fluid inclusion studies. Unpublished.

Sharp, I., Gillespie, P., Morsalnezhad, D., Taberner, C., Karpuz, R., Vergés, Horbury, J.A. Pickard, N., Garland, J., and Hunt, D., 2010. Stratigraphic architecture and fracture-controlled dolomitization of the Cretaceous Khami and Bangestan groups: an outcrop case study, Zagros Mountains, Iran. *Geological Society, London, Special Publications,* 329 (1), p.343-396. DOI: 10.1144/SP329.14

Shukri, F.F, 2010. *Characterization and origin of dolomite associated with hydrothermal iron ore in Palaeozoic Limestone, Kinta Valley.* Complete final year project.

Sibley, D.F. and Gregg, J.M., 1984. Epigenetic Dolomitization and the Origin of Xenotopic Dolomite Texture. *Journals of Sedimentary Petrology,* 54 (3), p.908-931. DOI: 10.1306/212F8535-2B24-11D7-8648000102C1865D

Singh, D. S., Chu, L. H., Teoh, L. H., Loganathan, P., Cobbing, E. J., Mallick, D. I. J., 1984. The Stong Complex: a reassessment. *Geological Society of Malaysia Bulletin,* 17, p.61-77. DOI: 0.7186/bgsm17198405

Sun, S. Q., 1994. A reappraisal of dolomite abundance and occurrence in the Phanerozoic: perspective. *Journal of Sedimentary Research,* A64 (2a), p.396-404. DOI: 10.1306/D4267DB1-2B26-11D7-8648000102C1865D

Suntharalingam, T., 1968. Upper Palaeozoic Stratigraphy of the Area West of kampar, Perak. *Geological Society of Malaysia, Bulletin,* 1, p.1-15.

Tucker, M.E., Wright, V.P., 1990. *Carbonate Sedimentology*. Blackwell Scientific Publication, Oxford.

Vuillemin, A., Ndiaye, M., Martini, R., and Davaud, E., 2011. Cement stratigraphy: image probes of cathodoluminescent facies. *Swiss Journal of Geosciences,* 104 (1), p.55-66.

Warren, J., 2000. Dolomite: occurrence, evolution and economically important as sociation. *Earth Science Review,* 52, p.1-81.

Wilson, M.E., Evans, M.J., Oxtoby, N.H., Nas, D.S., Donnelly, T., and Thirlwall, M., 2007. Reservoir quality, textural evolution, and origin of fault-associated dolomites. *American Association of Petroleum Geologists bulletin,* 91 (9), p.1247-1272.

Wong, T.W., 1991. Geology and mineral resources of the Lumut-Teluk Intan area, Perak Darul Ridzuan. *Geological Survey Map Report,* 3, p.1-96.

Zhu, D.C., Zhao, Z.D., Niu, Y., Dilek, Y., and Mo, X.X., 2011. Lhasa terrane in southern Tibet came from Australia. *Geology,* 39, p.727-730.